A Novel Analytical Method to Detect Adulteration of Virgin Olive Oil by Other Oils

T. Mavromoustakos[a,*], M. Zervou[a], G. Bonas[a], A. Kolocouris[a], and P. Petrakis[b]

[a]National Hellenic Research Foundation, Institute of Organic and Pharmaceutical Chemistry, 11635 Athens, Greece, and [b]Ministry of Agriculture & Forestry, Division of Informatics, Natural Resource Monitoring, 11143 Athens, Greece

ABSTRACT: The present study focuses on the olefinic region of the ^{13}C nuclear magnetic resonance (^{13}C NMR) spectrum of virgin olive oil which shows 12 peaks resonating between 127.5 and 130 ppm. These peaks are assigned to the most abundant unsaturated fatty acid moieties of the olive oil, oleic and linoleic acids, which are present in α and β positions of the glycerol backbone. With the use of an internal reference pyrazine, the 12 peaks were integrated and their areas were expressed in mmol/g of virgin olive oil. The intensities of the 12 observed peaks were affected when an authentic virgin olive oil was mixed with a seed oil. This observation was used to develop a semiquantitative method to detect adulteration of virgin olive oil by other oils based on ^{13}C NMR spectroscopy.

Paper no. J9247 in *JAOCS 77,* 405–411 (April 2000).

KEY WORDS: Adulteration, high-resolution ^{13}C NMR spectroscopy, virgin olive oil.

The composition of olive oil, and indeed of all vegetable oils, is generally defined in terms of the nature and distribution of the fatty acids present in the triacylglycerols and also of the positions at which these fatty acids are attached to the glycerol backbone. The acyl groups can be attached to the α (1,3-acyl) or β (2-acyl) position of the glycerol backbone. Olive oil contains mainly oleyl and linoleyl (unsaturated moieties) together with palmitic and stearic (saturated moieties) acyl groups. The considerable rise in consumer interest in olive oil as a healthful product and the economic premium attached, particularly to the highest-quality categories, increase the risks of adulteration with cheaper products.

Chromatographic methods currently used to detect adulteration of virgin olive oil (VO) by other oils suffer from many disadvantages. In particular, they are not specific, and they are destructive, time-consuming, and qualitative. Therefore, a method that overcomes these disadvantages would provide a means of easier and more precise detection of adulteration (1–3).

It has been recognized that ^{13}C nuclear magnetic resonance (NMR) spectroscopy is a valuable technique to analyze the most abundant fatty acids of various oils (4–7). Mavromoustakos *et al.* (8) report a quantitative analysis method for the most abundant fatty acids in olive oil using ^{13}C NMR. Reports in the literature point out that this technique may be useful in the detection of adulteration of VO by other oils (9,10). However, no systematic effort has been made to prove or disprove these statements. Therefore, the objective of this study was to use the ^{13}C NMR technique systematically to explore its capabilities in detecting adulteration of VO by other oils.

*To whom correspondence should be addressed at National Hellenic Research Foundation, Institute of Organic and Pharmaceutical Chemistry, 48 Vas. Constantinou Ave., 11635 Athens, Greece. E-mail: tmavro@eie.gr

EXPERIMENTAL PROCEDURES

Extra virgin olive oils. (i) Materials and sample preparation. The sample contained about 1 mL of authentic VO in $CDCl_3$ (40% w/w). A known mass (~15 mg) of 1,4 diazine (pyrazine) was added as an internal reference in a 5-mm NMR tube and mixed thoroughly.

(ii) Instrumentation and data processing. Spectra were recorded on a Bruker AC 300 spectrometer (Karlsruhe, Germany) operating at 75.46 MHz at a temperature of 313 K. This is an optimal temperature, where the best resolution was obtained without significant evaporation of the solvent. The inverse gated pulse program was used to give fully decoupled spectra with no nuclear Overhauser effect (NOE). The relaxation delay applied during the experiment was 44.6 s ($>5T_1$ of the slowest-relaxing nucleus) and the number of scans was 300. In order to obtain a high digital resolution (0.092 Hz/pt), which increases the precision of the peak simulation during analysis of the spectra, the time domain size of the free induction decay (FID) was set to 32 K and zero-filled to 128 K.

Processing of the FID and peak deconvolution of the spectra were carried out using the appropriate routines of one-dimensional WIN-NMR Bruker software. In particular, the FID is multiplied by the time function LG(t) which is defined as $LG(t) = EM(t)\cdot\exp[\pi\cdot LB\cdot(t_m^2 + t^2)/2t_m]$. EM($t$) stands for exponential multiplication and is given by the formula $EM(t) = \exp(-\pi\cdot LB\cdot t)$, and $t_m = GB\cdot taq$. GB is set to 20% of the recording acquisition time (taq) and LB is equal to the digital resolution and carries a negative sign (–0.092). Deconvolution of the spectra was performed using the automatic option provided in the Bruker software in order to avoid subjective human errors during the manual peak simulation. The best simulations were obtained by applying a Lorentzian-type curve fit to the olefinic peaks and Gaussian-type curve fit for the pyrazine peak.

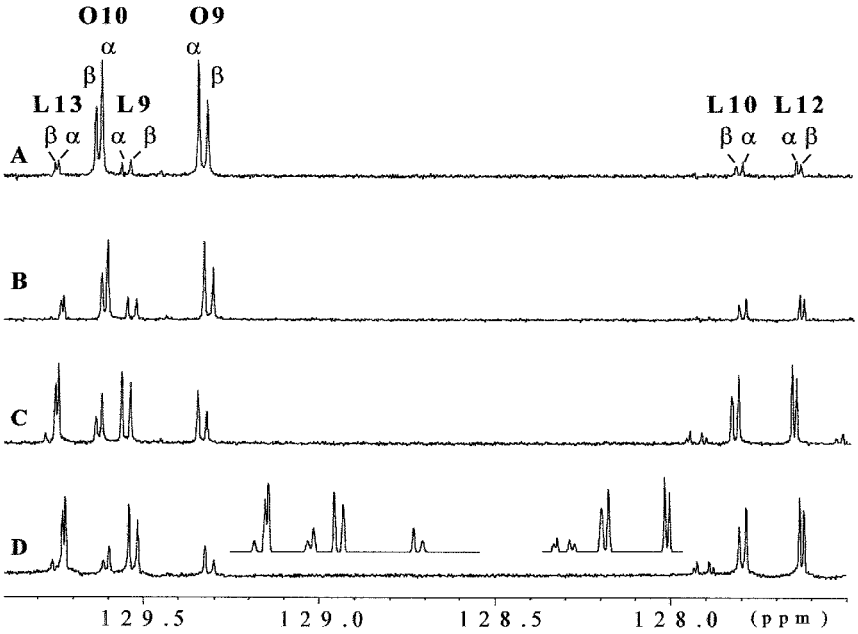

FIG. 1. ^{13}C nuclear magnetic resonance high-resolution spectra of the olefinic region of pure virgin olive oil and mixtures with soybean oil at 313 K recorded on an AC 300 MHz Bruker spectrometer (Karlsruhe, Germany). (A) Pure Greek virgin olive oil from Chania district located in Crete, (B) addition of 20% w/w soybean oil, (C) addition of 80% w/w soybean oil, and (D) pure soybean oil. The simulated spectrum is shown above line D. These peaks correspond to the ethylenic carbons of the oleic (O) and linoleic (L) moieties present in α and β positions of the glycerol backbone.

The olefinic region of the olive oil spectra consists of 12 distinct peaks resonating between 127.5 and 130 ppm. These peaks correspond to the ethylenic carbons of the oleic (O) and linoleic (L) moieties present in α and β positions of the glycerol backbone, namely O-9α, O-9β, O-10α, O-10β, L-9α, L-9β, L-10α, L-10β, L-12α, L-12β, L-13α, L-13β (Fig. 1A). The area of each peak is expressed in mmol of fatty acid moiety per g of oil using a known mass of pyrazine as an internal reference.

Our study focused on the olefinic region because it contains fewer overlapped peaks when compared to the carbonylic region of the spectrum. Therefore, the simulation of these peaks gives the most accurate results, which are comparable to the gas chromatography data (8).

To quantify the obtained NMR data, the area of a particular peak was directly compared to the area of the pyrazine peak which corresponds to a known mass content expressed in mmol. Pyrazine gives only a single peak at a chemical shift of 144.8 ppm. Thus, this peak is close to the region of interest and does not coincide with any of the observed peaks.

The mass content of a given peak is then normalized to 1 g of oil. The formula used to express the results in mmol/g is:

$$X_i \text{ (mmol/g)} = 4 \times (W_p/\text{MW}_p) \times (S_i/S_p) \times (1000/W_{\text{oil}}) \qquad [1]$$

where W_p (mg) is the weight of pyrazine added, MW_p is the molecular weight of pyrazine, W_{oil} (mg) is the weight of oil (or mixtures of oils), S_i is the area of the individual peak calculated after deconvolution of the peaks, and S_p is the area of the pyrazine peak calculated also after deconvolution. The factor four is used to normalize over the four magnetically equivalent pyrazine carbon atoms.

The calculated oleic and linoleic content of the 61 extra virgin olive oil samples obtained after integrating four representative olefinic peaks (O-10α, L-9α, O-9α, L-10α) are shown in Table 1. These obtained values will be called "diagnostic parameters" in this paper.

Mixtures of extra virgin olive oils with seed oils. The same methodology was applied in a new series of experiments with samples containing VO adulterated with several levels of seed oil. In all samples, a 40% w/w concentration of the mixture in the chloroform solution was used to obtain comparable results. The seed oils used were soybean oil (SO), cottonseed oil (CsO), corn oil (CoO), and sunflower seed oil (SuO). By using the same diagnostic parameters, the calculated content of the unsaturated fatty acid moieties in mmol/g for the examined mixtures of VO with seed oils is also given in Table 1. The pure VO along with the adulterated samples are divided into 13 groups (0, 5, 10, 15, 20, 25, 30, 35, 40, 45, 60, 80, 100) according to the percentage of adulteration.

Statistical evaluation. Discriminant analysis was performed for the database samples, consisting of authentic or adulterated VO (11). The analysis is based (i) on the derivation of statistically significant discriminant functions and (ii) on the separators of group regions characterized by group centroids (territorial map). The territorial map is used as

nomogram for the allocation of new samples in groups (12). The samples are positioned in the territorial map according to their discriminant scores.

RESULTS AND DISCUSSION

This study is based on the analysis of 61 authentic Greek VO samples directly collected from oil mills and covering all major olive oil-producing areas of Greece. The sample collection was held in three consecutive harvest periods between the years 1994 and 1996. A questionnaire was completed right after collection in the mills, containing information on the cultivar, climatic conditions, altitude of the olive grove, agronomic conditions, harvesting and extracting methods, installation type, and processing conditions. As it will be discussed later, these factors were examined in an effort to understand their influence on the obtained data. This study is also based on the analysis of several seed oils (SO, CoO, CsO, and SuO) as well as their mixtures with authentic VO.

The total sample set served as a database to test the capability of high-resolution ^{13}C NMR spectroscopy to detect adulteration of VO by other oils. The method is based on the area integration of each observed peak in the olefinic region. The addition of adulterants affects the area of each of the observed olefinic peaks. Therefore, the quantitative determination of the most abundant fatty acid moieties by ^{13}C NMR spectroscopy leads to a valuable method that quantitatively detects the adulteration of VO by other oils. This novel method is not destructive since it involves only dissolution of the olive oil sample in a deuterated chloroform solvent.

^{13}C NMR spectra of VO and its mixtures with seed oils. The olefinic region of the ^{13}C NMR high-resolution spectrum of a VO is shown in Figure 1 (spectrum A). The sample originates from the Chania district of Crete, a major olive oil-producing area. Spectra B and C were obtained from the same authentic VO sample mixed with SO at increasing concentrations while spectrum D shows the spectrum obtained from pure SO.

Two of the major features observed in the series of spectra of Figure 1 are these: (i) As the relative concentration of SO increased, a corresponding increase in the intensities of the linoleic acid peak and a decrease in the intensities of the oleic acid peak were observed. This is due to the fact that VO contains an average of 73% oleic and 7% linoleic acids whereas SO contains 23% oleic and 54% linoleic acids. (ii) Additional peaks resonating at 127.9 ppm appear in spectra C and D, suggesting that the newly formed peaks are due to the presence of SO and detection can be completed through a visual inspection.

Construction of reference curves. The linoleic acid content (mmol/g) for an authentic VO sample from Chania district and its mixtures with increasing amounts of seed oils (adulteration levels 5–100%) is plotted (Fig. 2). The following observations can be deduced: (i) There is a linear increase in linoleic acid as the level of seed oil adulteration increases. This is attributed to the fact that the seed oils used in this study have higher percentages of linoleic acid compared to

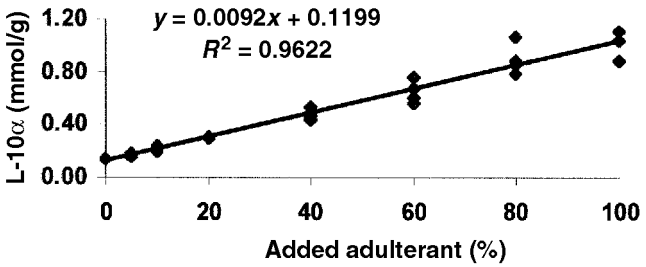

FIG. 2. Linear variation of L-10α in mmol/g as the percentage of adulteration increases. For abbreviation see Figure 1.

VO. On the other hand, a linear decrease in the oleic acid is observed as the seed oil adulteration increases owing to the fact that seed oils contain lower percentages of oleic acid. (ii) Detection of adulteration through inspection of the linoleic acid content (mmol/g) is possible when the percentage of adulteration is ≥5%. Curves for other diagnostic parameters can be constructed using data provided by Table 1. A linear response was observed when the 12 olefinic parameters were used, of which the eight referring to linoleic acid appeared more diagnostic than those of oleic acid.

Other curves constructed for authentic samples originating from other regions in Greece and using the same adulterants showed similar results. By using the above reference curves it is possible to verify the authenticity or to estimate the adulteration of a VO sample.

Such curves were not useful as a diagnostic tool for low percentages of adulteration (5–15%) where the origin of the oil or the adulterant was unknown. The amount of rainfall in an area, the location of the field (such as near a road, near the sea, in a mountainous area) and the altitude of the field (plain, mid-mountain, mountain) affect the chemical composition of the fatty acids of the oil; thus, variation in the oil may not be diagnosed correctly. Factors related to the processing of oil (such as the paste temperature), the degree of ripeness, or the variety of the olives in the fields (koroneiki, psiloelia, chondroelia, etc.) were found to affect the chemical composition of the fatty acids of the oil. However, a definite trend in the way these factors affect the chemical composition of the olive oil was not established. It appears that at least all the abovementioned factors determine the specific chemical profile of the olive oil. A support of this view is provided in a recent report by Vlahov *et al.* (13).

Statistical analysis. Because of the diversity of factors that affect the fatty acid distribution of the oil, a statistical treatment is necessary to improve the diagnostic power of analysis. The reference curves (a representative one is shown in Fig. 2) are in this case substituted to a multivariate analog that corresponds to a territorial map constructed on the basis of two or more composite axes from the entire set of diagnostic variables. Therefore, discriminant analysis was used to approach this problem using the described database of samples.

Only the first two discriminant functions (DF1 and DF2) were deemed significant (Wilk's lambda = 0.215, $x^2 = 19.199$, $P < 0.0005$). Figure 3 shows a plot of DF2 vs. DF1. The vari-

TABLE 1
Quantitative ^{13}C Nuclear Magnetic Resonance Data on Simulated Areas of 4 Out of 12 Observed Olefinic Peaks Using 61 Authentic Greek Virgin Olive Oil Samples and 78 Mixtures of Virgin Olive Oil with Seed Oils[a]

S/N	Origin	O-10α	L-9α	O-9α	L-10α	S/N	Oil origin	Adulterant[b]	O-10α	L-9α	O-9α	L-10α
1	Chania	1.4397	0.1260	1.3991	0.1463	1	Chania	5% CsO	1.3225	0.1651	1.3150	0.1790
2	Chania	1.2173	0.1209	1.2379	0.1010	2	Chania	5% SuO	1.3114	0.2008	1.2773	0.1854
3	Lakonia	1.4681	0.1543	1.5251	0.1339	3	Chania	5% SO	1.2360	0.1884	1.2142	0.1647
4	Lakonia	1.3288	0.1878	1.2790	0.1720	4	Chania	5%CoO	1.3084	0.1405	1.3417	0.1581
5	Messinia	1.4321	0.1229	1.4101	0.0951	5	Lakonia	5% SO	1.1761	0.2071	1.1796	0.1750
6	Messinia	1.2431	0.1244	1.3037	0.1120	6	Lakonia	5% CsO	1.2159	0.2074	1.2201	0.2062
7	Etol/nia	1.4922	0.0711	1.4772	0.0765	7	Lakonia	5% CoO	1.3158	0.2088	1.2948	0.2075
8	Evia	1.2191	0.2470	1.1808	0.2568	8	Lakonia	5% SuO	1.2168	0.2020	1.1962	0.2146
9	Fthiotida	1.3011	0.1382	1.2892	0.1376	9	Heraklion	5.1% CsO	1.1495	0.0972	1.1394	0.1133
10	Zakinthos	1.3889	0.1242	1.4174	0.1168	10	Chania	5.55% CsO	1.1793	0.1122	1.2054	0.1220
11	Lesvos	1.2396	0.1749	1.2399	0.1850	11	Messinia	6.04% CoO	1.1673	0.1045	1.1694	0.1122
12	Chania	1.3841	0.0690	1.3925	0.0822	12	Chania	10% CoO	1.1831	0.2466	1.1849	0.1941
13	Chania	1.2779	0.1203	1.3238	0.0734	13	Chania	10% SO	1.3662	0.2352	1.3331	0.2315
14	Chania	1.3542	0.0673	1.3991	0.0785	14	Chania	10% CsO	1.2406	0.2097	1.2088	0.2039
15	Chania	1.2267	0.0698	1.2382	0.0769	15	Chania	10% SuO	1.1487	0.2213	1.1144	0.2024
16	Heraklion	1.2925	0.0968	1.3658	0.0910	16	Lakonia	10% SuO	1.2570	0.2661	1.2406	0.2574
17	Heraklion	1.3018	0.0934	1.3367	0.0794	17	Lakonia	10% CsO	1.2180	0.2710	1.2703	0.2396
18	Heraklion	1.2755	0.0810	1.3447	0.0731	18	Lakonia	10% SO	1.1924	0.2229	1.1669	0.2352
19	Heraklion	1.1650	0.0815	1.1684	0.0773	19	Lakonia	10% CoO	1.3834	0.2864	1.2658	0.2597
20	Heraklion	1.2253	0.0968	1.2398	0.0973	20	Heraklion	9.81% SuO	1.1440	0.1654	1.1348	0.1412
21	Lassithi	1.1750	0.0772	1.1782	0.0976	21	Heraklion	10.15% CsO	1.1064	0.1475	1.1064	0.1450
22	Lassithi	1.2185	0.0791	1.2206	0.0817	22	Heraklion	10.8% SO	1.1588	0.1490	1.1878	0.1372
23	Heraklio	1.1369	0.0650	1.1645	0.0708	23	Chania	16.33% SuO	1.1601	0.2272	1.1702	0.2230
24	Lassithi	1.2118	0.0546	1.2308	0.0568	24	Chania	17.91% SuO	1.1688	0.3148	1.1809	0.2544
25	Lassithi	1.1644	0.1504	1.2191	0.1354	25	Chania	16.13% CsO	1.3291	0.2800	1.4008	0.2229
26	Lassithi	1.2227	0.1150	1.2317	0.1031	26	Chania	16.61% CsO	1.3464	0.3146	1.2441	0.2350
27	Lassithi	1.1923	0.1144	1.2148	0.1167	27	Chania	15.49% CsO	1.5606	0.3130	1.5275	0.2400
28	Lassithi	1.2592	0.1366	1.2664	0.1247	28	Chania	15.49% CsO	1.4074	0.2426	1.5155	0.2347
29	Korinthia	0.8771	0.0968	0.9078	0.0840	29	Korinthia	16.63% CsO	1.0517	0.2087	1.0506	0.1959
30	Korinthia	1.2825	0.1098	1.2656	0.0687	30	Chania	17.22% CoO	1.1422	0.1547	1.1450	0.2030
31	Korinthia	1.3159	0.0737	1.3386	0.0753	31	Chania	20% CoO	1.1682	0.2925	1.1473	0.2965
32	Korinthia	1.4017	0.1859	1.4484	0.1591	32	Chania	20% SO	1.1392	0.3220	1.2112	0.3029
33	Argolida	1.2266	0.1870	1.2829	0.1564	33	Chania	20% CsO	1.1119	0.3006	1.1186	0.3024
34	Argolida	0.9839	0.2477	0.9907	0.2216	34	Lakonia	20% SuO	1.1530	0.3740	1.1541	0.3628
35	Arkadia	1.3289	0.1425	1.3334	0.1403	35	Lakonia	20% CsO	1.1457	0.3508	1.1395	0.3392
36	Lakonia	1.5252	0.1027	1.4949	0.0905	36	Lakonia	20% SO	1.1571	0.3338	1.1872	0.3227
37	Lakonia	1.4246	0.0851	1.3764	0.1120	37	Lassithi	19.9% SuO	1.0810	0.2339	1.0300	0.2176
38	Lakonia	1.2632	0.1122	1.2730	0.0901	38	Messinia	20.29% SuO	1.0731	0.2900	1.0669	0.2612
39	Lakonia	0.9713	0.0627	1.0054	0.0543	39	Lakonia	10.87% SO + 3.7% CoO + 5.5% SuO	1.0877	0.2032	1.0877	0.2292
40	Lakonia	1.2165	0.0920	1.2535	0.0929	40	Chania	11.71% SuO + 12.54% SO	1.0671	0.2091	1.0681	0.2626
41	Lakonia	1.1111	0.1345	1.1375	0.1362	41	Chania	24.37% CsO	1.0370	0.1456	1.0294	0.2422
42	Lakonia	1.3992	0.0613	1.3736	0.0828	42	Messinia	14.21% CsO + 15.62% CoO	0.9700	0.2857	1.0034	0.2942
43	Messinia	1.3071	0.1308	1.3708	0.1177	43	Messinia	30.02% SuO	0.9872	0.3307	0.9928	0.3279
44	Messinia	1.3156	0.0768	1.3019	0.0616	44	Messinia	30.02% SuO	0.9539	0.3219	0.9724	0.3224
45	Messinia	1.2830	0.0974	1.2826	0.0879	45	Argolida	30.4% CoO	0.8315	0.3365	0.8260	0.3251
46	Messinia	1.3546	0.1013	1.3688	0.0833	46	Argolida	30.4% CoO	0.9262	0.3545	0.8820	0.3645
47	Messinia	1.3098	0.0785	1.3166	0.1012	47	Ilia	29.6% SO	1.0092	0.3119	0.9896	0.2635
48	Messinia	1.1148	0.0851	1.0949	0.0736	48	Korinthia	34.9% CoO	0.9010	0.3537	0.9155	0.3400
49	Messinia	1.2263	0.0613	1.2327	0.0733	49	Chania	40% CoO	0.9169	0.4474	0.9255	0.4386
50	Achaia	1.3933	0.1629	1.4203	0.0922	50	Chania	40% SO	0.9843	0.4529	0.9894	0.4568
51	Evia	1.1758	0.1576	1.1698	0.1389	51	Chania	40% CsO	1.0238	0.4881	1.0241	0.4902
52	Evia	1.3176	0.1492	1.3164	0.1418	52	Chania	40% SuO	0.9688	0.5380	0.9633	0.5283
53	Zakinthos	1.4517	0.1283	1.4525	0.1053	53	Lakonia	40% SuO	0.8706	0.4923	0.9088	0.4859
54	Rodos	1.1859	0.2281	1.2193	0.2206	54	Lakonia	40% CsO	0.9859	0.5295	1.0209	0.4974
55	Lesvos	1.4492	0.0855	1.4118	0.1178	55	Lakonia	40% SO	0.7499	0.6163	0.7495	0.5768
56	Lesvos	1.3041	0.1902	1.2869	0.1735	56	Rethimno	39.86% CoO	0.7583	0.3152	0.7540	0.3175
57	Lesvos	1.2453	0.1335	1.2289	0.1467	57	Messinia	44.75% CoO	0.9487	0.3976	0.9746	0.4082
58	Lesvos	1.1469	0.1094	1.1693	0.1070	58	Chania	60% CoO	0.7557	0.6103	0.7814	0.6006
59	Lesvos	1.3825	0.1469	1.3537	0.1521	59	Chania	60% SO	0.7501	0.5908	0.7580	0.5525
60	Chalkidiki	1.3651	0.0766	1.3622	0.0852	60	Chania	60% CsO	0.9018	0.6877	0.9227	0.6722
61	Chalkidiki	1.3091	0.1176	1.2964	0.1422	61	Chania	60% SuO	0.8598	0.7534	0.8512	0.7477

(continued on next page)

TABLE 1 (continued)

S/N	Origin	O-10α	L-9α	O-9α	L-10α	S/N	Oil origin	Adulterant[b]	O-10α	L-9α	O-9α	L-10α
						62	Lakonia	60% SuO	0.8740	0.7830	0.8875	0.7729
						63	Lakonia	60% CsO	0.8696	0.6919	0.8535	0.6902
						64	Lakonia	60% SO	0.7695	0.6384	0.7873	0.5928
						65	Chania	80% CoO	0.6381	0.9148	0.6522	0.8729
						66	Chania	80% SO	0.6580	0.7706	0.6447	0.7839
						67	Chania	80% CsO	0.7271	0.8775	0.7206	0.8453
						68	Chania	80% SuO	0.7485	1.0763	0.7841	1.0549
						69	Lakonia	80% SuO	0.7067	1.0068	0.6873	0.9590
						70	Lakonia	80% CsO	0.6306	0.7865	0.6297	0.7937
						71	Lakonia	80% SO	0.6030	0.7937	0.6268	0.7708
						72		CoO	0.3000	0.8889	0.3273	0.8798
						73		SO	0.4938	0.9715	0.4400	1.0318
						74		SuO	0.4909	1.1066	0.4732	1.0956
						75		CsO	0.5586	1.1224	0.6211	1.0959
						76		SO (commercial)	0.3978	0.8757	0.3727	0.8688
						77		SuO (commercial)	0.3974	1.1001	0.3955	1.1184
						78		CsO (commercial)	0.2573	0.8245	0.2779	0.8316

[a]Areas are expressed in mmol/g of oil.
[b]CsO, cottonseed oil; SuO, sunflowerseed oil; SO, soybean oil; CoO, corn oil. See text for explanation of O-10α, L-9α, O-9α, and L-10α.

ables that exhibit the highest correlation with the discriminant functions are shown in Table 2. The first discriminant function is associated with the linoleic acid whereas the second characterizes the oleic acid. The α position seems sufficient in separating oil sample groups, and the linoleic acid appears sufficient to distinguish the samples.

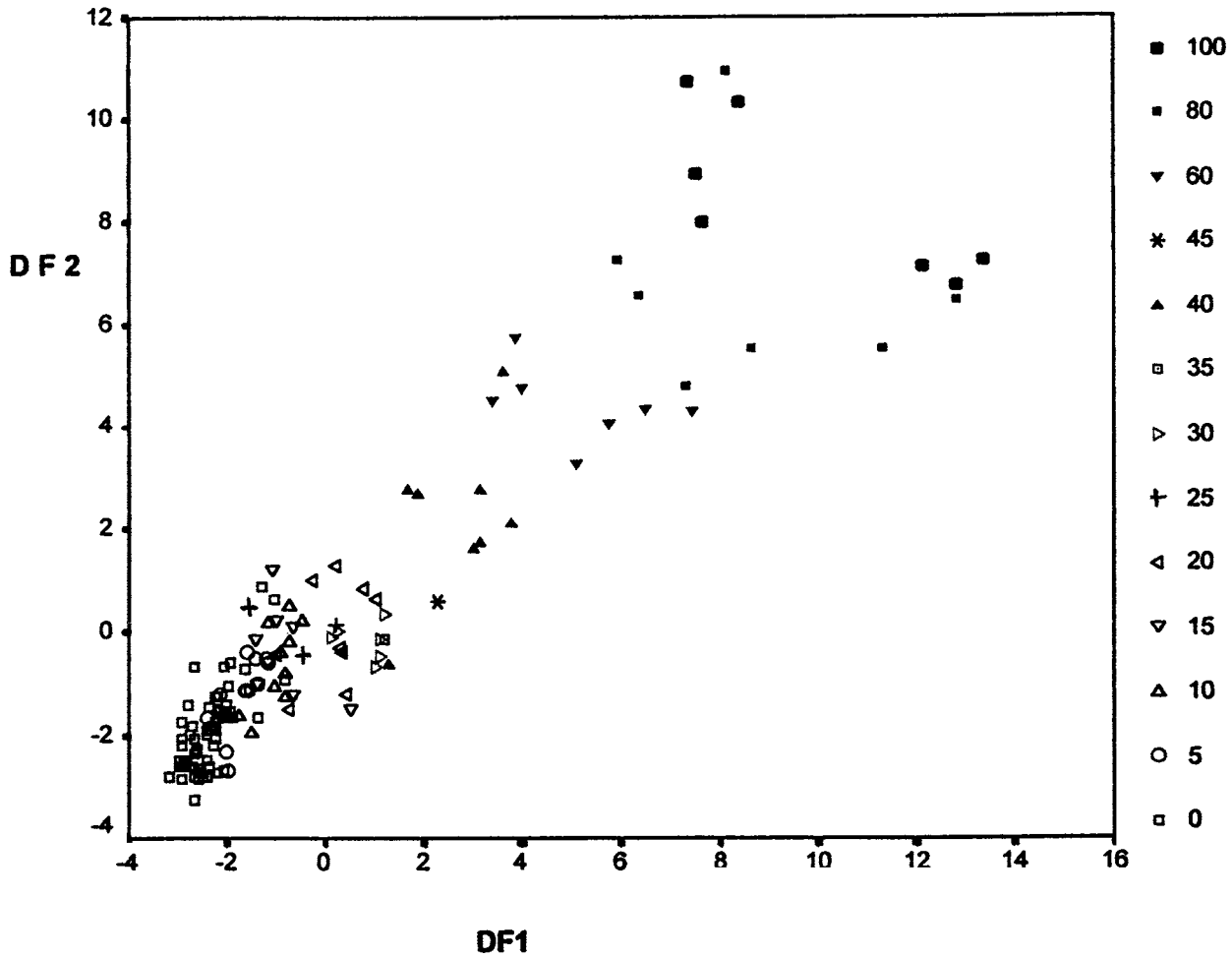

FIG. 3. Plot of discriminant function 1 (associated with the linoleic acid) vs. discriminant function 2 (associated with the oleic acid).

TABLE 2
Rotated Structure Matrix[a]

Variable	DF1[b]	DF2[b]
L-10α	.986*	.061
L-9α	.975*	.101
L-12α	.946*	.107
L-10β	.720*	.011
L-12β	.679*	–.112
L-13α	.676*	.081
L-9β	.629*	.131
L-13β	.486*	.040
O-9α	.119	.992*
O-10α	.137	.945*
O-10β	–.021	.899*
O-9β	.015	.888*

[a]Variables are ordered by the size of correlation within function.
[b]The asterisks show the largest absolute correlation between each variable and any discriminant function.

The appropriate classification results showing the predicted group membership for all original groups are shown in Table 3. The first row and column in Table 3 correspond to the 13 groups, and the diagonal elements represent the percentage of the correctly classified groups. By inspecting each row separately one can realize the predictive power of the method. For example, the first row shows that 78.5% of the VO samples are classified correctly, 15.4 and 4.6% were misclassified as 5 or 20% adulterated, respectively. By using the same analysis for all rows the following conclusions can be derived.

(i) The method is 100% successful when levels of >40% are used. For mixtures ≤40% the method has an 80% success rate in correctly classifying the adulteration level. Also, the misclassification is limited to groups that differ mainly by ±5% adulteration level.

(ii) All the adulterated samples were detected correctly in a qualitative sense. Thus, none of the adulterated samples was misclassified as authentic. The novel method is useful not only for classifying a sample as adulterated or authentic but also for quantitatively giving an estimate of the degree of adulteration.

(iii) Cross-validated values express the misclassification percentages of samples when groups are constructed in the absence of the sample group under consideration. The percentages of classification are not significantly reduced. This is *a posteriori* justification of the fact that the entire set of samples is capable of predicting group affiliation of unknown samples and in this way serves as an examination tool of VO adulteration.

In particular, cross-validation values (not shown) for authentic VO showed only a small percentage reduction when compared with those reported in Table 3. In some adulteration levels, the reduction was high but this was caused by the misclassification limited only by ±5%. As an example, the highest reduction was observed in the cross-validation number of the 5% adulteration level (75.0 vs. 41.7%). However, this reduction was only due to 5% misclassification (33.3% were misclassified as authentic).

ACKNOWLEDGMENTS

This study was supported by contract grant number AIR2-CT PL941224 of the European Commission. The authors acknowledge Dr. Anastassios Helmis (Elais) who provided us the authentic VO samples as well as the experienced collectors of the same company who gathered the samples from the mills and completed the questionnaire. The authors thank the reviewers for their constructive criticisms of the manuscript.

REFERENCES

1. Kapoulas, V.M., and S. Passaloglou-Emmanouilidou, Detection of Adulteration of Olive Oil with Seed Oils by a Combination of Column and Gas Liquid Chromatography, *J. Am. Oil Chem. Soc. 58*:694–697 (1981).
2. Rossell, J.B., B. King, and M.J. Downes, Detection of Adulteration, *Ibid. 60*:333–339 (1983).
3. Kiritsakis, A., and P. Martakis, Olive Oil Analysis, *Mod. Methods Plant Anal. New Ser. 12*:1–20 (1991).
4. Gunstone, F.D., The Composition of Hydrogenated Fats by

TABLE 3
Classification Results Showing the Predicted Group Membership for the Original Groups

Origin	0	5	10	15	20	25	30	35	40	45	60	80	100	Total
0	**78.5**	15.4	1.5	.0	4.6	.0	.0	.0	.0	.0	.0	.0	.0	100.0
5	.0	**75.0**	25.0	.0	.0	.0	.0	.0	.0	.0	.0	.0	.0	100.0
10	.0	18.2	**81.8**	.0	.0	.0	.0	.0	.0	.0	.0	.0	.0	100.0
15	.0	.0	12.5	**50.0**	25.0	12.5	.0	.0	.0	.0	.0	.0	.0	100.0
20	.0	.0	.0	.0	**100.0**	.0	.0	.0	.0	.0	.0	.0	.0	100.0
25	.0	.0	.0	.0	.0	**100.0**	.0	.0	.0	.0	.0	.0	.0	100.0
30	.0	.0	.0	.0	.0	.0	**100.0**	.0	.0	.0	.0	.0	.0	100.0
35	.0	.0	.0	.0	.0	.0	.0	**100.0**	.0	.0	.0	.0	.0	100.0
40	.0	.0	.0	.0	.0	.0	12.5	.0	**75.0**	.0	12.5	.0	.0	100.0
45	.0	.0	.0	.0	.0	.0	.0	.0	.0	**100.0**	.0	.0	.0	100.0
60	.0	.0	.0	.0	.0	.0	.0	.0	.0	.0	**100.0**	.0	.0	100.0
80	.0	.0	.0	.0	.0	.0	.0	.0	.0	.0	.0	**100.0**	.0	100.0
100	.0	.0	.0	.0	.0	.0	.0	.0	.0	.0	.0	.0	**100.0**	100.0

[a]The first row and column correspond to the 13 groups while the diagonal elements represent the percentage of the correctly classified groups.

High-Resolution ^{13}C Nuclear Magnetic Resonance Spectroscopy, *J. Am. Oil Chem. Soc. 70*:965–970 (1993).
5. Knothe, G., M.S.F. Lie Ken Jie, C.C. Lam, and M.O. Bagby, Evaluation of the ^{13}C-NMR Signals of the Unsaturated Carbons of Triacylglycerols, *Chem. Phys. Lipids 77*:187–191 (1995).
6. Wollenberg, K.F., Quantitative High Resolution ^{13}C Nuclear Magnetic Resonance of the Olefinic and Carbonyl Carbons of Edible Vegetable Oils, *J. Am. Oil Chem. Soc. 67*:487–494 (1990).
7. Zamora, R., J.L. Navarro, and F. Hidalgo, Identification and Classification of Olive Oils by High Resolution ^{13}C Nuclear Magnetic Resonance, *Ibid. 71*:361–364 (1994).
8. Mavromoustakos, T., M. Zervou, E. Theodoropoulou, D. Panagiotopoulos, G. Bonas, and A. Helmis, A ^{13}C NMR Analysis of the Triacylglycerol Composition of Greek Virgin Olive Oils, *Magn. Reson. Chem. 35*:S3–S7 (1997).
9. Sacchi, R., F. Addeo, and L. Paolillo, ^{1}H and ^{13}C NMR of Virgin Olive Oil. An Overview, *Ibid. 35*:S133–S145 (1997).
10. Vlahov, G., Improved Quantitative ^{13}C Nuclear Magnetic Resonance Criteria for Determination of Grades of Virgin Olive Oils. The Normal Ranges for Diglycerides in Olive Oil, *J. Am. Oil Chem. Soc. 73*:1201–1203 (1996).
11. Morrison, D.F., *Multivariate Statistical Methods*, McGraw-Hill, New York, 1984, pp. 274.
12. Legendre, L., and P. Legendre, *Numerical Ecology*, Elsevier, Amsterdam, 1979, pp. 360–380.
13. Vlahov, G., A.D. Shaw, and D.B. Kell, Use of ^{13}C Nuclear Magnetic Resonance Distortionless Enhancement by Polarization Transfer Pulse Sequence and Multivariate Analysis to Discriminate Olive Oil Cultivars, *J. Am. Oil Chem. Soc. 76*:1223–1231 (1999).

[Received May 17, 1999; accepted January 21, 2000]